Signal Transduction:

Mechanistic Insights into Allosteric Structure-Function Relationships at the M 1 Muscarinic Acetylcholine Receptor

Alaa Abdul-Ridha, J. Robert Lane, Shailesh N. Mistry, Laura López, Patrick M. Sexton, Peter J. Scammells, Arthur Christopoulos and Meritxell Canals

J. Biol. Chem. 2014, 289:33701-33711.
doi: 10.1074/jbc.M114.604967 originally published online October 17, 2014

THE JOURNAL OF BIOLOGICAL CHEMISTRY VOL. 289, NO. 48, pp. 33701–33711, November 28, 2014

Mechanistic Insights into Allosteric Structure-Function Relationships at the M_1 Muscarinic Acetylcholine Receptor*[S]

Received for publication, August 19, 2014, and in revised form, October 6, 2014 Published, JBC Papers in Press, October 17, 2014, DOI 10.1074/jbc.M114.604967

Alaa Abdul-Ridha[‡1,2], J. Robert Lane[‡1,3], Shailesh N. Mistry[§], Laura López[‡], Patrick M. Sexton[‡4], Peter J. Scammells[§], Arthur Christopoulos[‡4,5], and Meritxell Canals[‡6]

From the Departments of [‡]Drug Discovery Biology and [§]Medicinal Chemistry, Monash Institute of Pharmaceutical Sciences and Department of Pharmacology, Monash University, Parkville, Victoria 3052, Australia

Background: Selective and potent positive allosteric modulators (PAMs) of the M_1 mAChR have been recently described.
Results: Use of structural analogues and mutagenic mapping identified the mechanistic basis for increased PAM activity.
Conclusion: Combined analytical, structure-function, and modeling approaches uncover allosteric mechanisms at the M_1 mAChR.
Significance: New chemical space can be explored in the development of tailored M_1 mAChR PAMs.

Benzylquinolone carboxylic acid (BQCA) is the first highly selective positive allosteric modulator (PAM) for the M_1 muscarinic acetylcholine receptor (mAChR), but it possesses low affinity for the allosteric site on the receptor. More recent drug discovery efforts identified 3-((1*S*,2*S*)-2-hydroxycyclohexyl)-6-((6-(1-methyl-1*H*-pyrazol-4-yl)pyridin-3-yl)methyl)benzo[*h*]-quinazolin-4(3*H*)-one (referred to herein as benzoquinazolinone 12) as a more potent M_1 mAChR PAM with a structural ancestry originating from BQCA and related compounds. In the current study, we optimized the synthesis of and fully characterized the pharmacology of benzoquinazolinone 12, finding that its improved potency derived from a 50-fold increase in allosteric site affinity as compared with BQCA, while retaining a similar level of positive cooperativity with acetylcholine. We then utilized site-directed mutagenesis and molecular modeling to validate the allosteric binding pocket we previously described for BQCA as a shared site for benzoquinazolinone 12 and provide a molecular basis for its improved activity at the M_1 mAChR. This includes a key role for hydrophobic and polar interactions with residues Tyr-179, in the second extracellular loop (ECL2) and Trp-400$^{7.35}$ in transmembrane domain (TM) 7. Collectively, this study highlights how the properties of affinity and cooperativity can be differentially modified on a common structural scaffold and identifies molecular features that can be exploited to tailor the development of M_1 mAChR-targeting PAMs.

G protein-coupled receptors (GPCRs)[7] are the largest class of cell surface receptors and mediate major physiological processes. With over 800 GPCRs encoded by the human genome, they are the target of more than 30% of currently marketed drugs (1). The M_1 mAChR is one of five muscarinic receptor subtypes that belong to the family A GPCRs (2). Numerous drug discovery efforts have focused on developing selective ligands for this receptor subtype as potential therapies for neurocognitive disorders, such as Alzheimer's disease and schizophrenia (3, 4). Efforts aimed at targeting the highly conserved orthosteric (ACh) binding site have largely failed because of a lack of ligand subtype selectivity, whereas those targeting topographically distinct allosteric sites have proven more fruitful (5, 6). However, allosteric ligands can display complex behaviors, modulating orthosteric ligand affinity or efficacy and/or displaying direct agonism in their own right. A surge in family A GPCR crystal structures has provided considerable insights into the location of orthosteric binding pockets and the molecular mechanisms underlying ligand binding and receptor activation (7, 8). Of particular interest, the recent solution of a crystal structure of the M_2 mAChR co-bound with an allosteric modulator and an orthosteric agonist has given the first snapshot of a mechanism by which a modulator can act to enhance orthosteric agonist affinity (9). However, such information is currently lacking for other GPCRs, and both the structural and dynamic bases of how allosteric modulation is transmitted between spatially distinct binding sites remain largely unexplored. Thus, a combination of structure-activity and structure-function studies of GPCR allostery remains a vital approach to addressing some of these challenges, provided that this approach is enriched by analytical methods that can dissect

* This work was funded by National Health and Medical Research Council of Australia Program Grants APP1055134 (to A. C. and P. M. S.) and APP1049564 (to J. R. L.). The computational studies were supported by resource allocation scheme Grant VR0024 of the Victorian Life Sciences Computation Initiative on its Peak Computing Facility at the University of Melbourne.
[S] This article contains supplemental materials.
[1] These authors contributed equally to this work.
[2] Recipient of an Australian Postgraduate Award scholarship.
[3] R.D. Wright NHMRC Career Development Fellow.
[4] Principal Research Fellows of the National Health and Medical Research Council of Australia.
[5] To whom correspondence may be addressed: Drug Discovery Biology, Monash Inst. of Pharmaceutical Sciences, Monash University, 381 Royal Parade, Parkville, Victoria 3052, Australia. Tel.: 03-9903-9067; Fax: 03-9903-9581; E-mail: arthur.christopoulos@monash.edu.
[6] M.C. is a Monash Fellow. To whom correspondence may be addressed: Drug Discovery Biology, Monash Inst. of Pharmaceutical Sciences, Monash University, 381 Royal Parade, Parkville, Victoria 3052, Australia. Tel.: 03-9903-9067; Fax: 03-9903-9581; E-mail: meri.canals@monash.edu.

[7] The abbreviations used are: GPCR, G protein-coupled receptor; ACh, acetylcholine; ANOVA, analysis of variance; BQCA, benzylquinolone carboxylic acid; CCh, carbachol; mAChR, muscarinic acetylcholine receptor; TM, transmembrane domain; NMS, *N*-methylscopolamine.

structural effects on ligand binding from transmission of cooperativity and receptor activation.

In a recent study, we combined site-directed mutagenesis, analytical modeling, and molecular dynamics to delineate regions of the M_1 mAChR governing actions of the prototypical positive allosteric modulator, BQCA (10). This compound has emerged as a useful tool because it displays absolute subtype selectivity for the M_1 mAChR, has a very high positive cooperativity with ACh, displays a mechanism of action that appears in strict accordance with a simple two-state model of receptor activity (11), and has shown *in vivo* efficacy (6, 12). We identified several residues that contribute to the BQCA binding pocket as well as to the transmission of cooperativity with the orthosteric agonist, carbachol. Such residues were located in the ECL2 and at the top of TM2 and TM7. The BQCA binding pocket was proposed to partially overlap with the previously described "common" allosteric site in the extracellular vestibule of mAChRs (9, 13–16), suggesting that its high subtype selectivity derives from either additional contacts outside this region or through a subtype-specific cooperativity mechanism (17).

Unfortunately, both the therapeutic utility of BQCA and potential for deeper mechanistic insights into M_1 mAChR allostery afforded by this molecule remain limited, because BQCA has a very low affinity for the M_1 mAChR in the absence of co-bound agonist (11) and poor aqueous solubility. This has mechanistic implications in that it limits the ability to utilize loss of function mutagenesis approaches to distinguish key residues that govern modulator affinity (thus directly contributing to the allosteric binding site) *versus* residues that contribute to the transmission of the allosteric effect (thus indirectly contributing to the observed potency and selectivity). Such insights would be greatly facilitated by the availability of higher affinity allosteric probes. Encouragingly, recent drug discovery efforts resulted in the disclosure of putative allosteric M_1 mAChR ligands with higher functional potency than BQCA, although the mechanism of action remains to be definitively established for a number of these compounds (18–23). One such compound, 3-((1*S*,2*S*)-2-hydroxycyclohexyl)-6-((6-(1-methyl-1*H*-pyrazol-4-yl)pyridin-3-yl)methyl)benzo[*h*]quinazolin-4(3*H*)-one, referred to herein as benzoquinazolinone 12 (see Fig. 1), is of particular interest, because it is structurally derived from BQCA but has been reported to have substantially higher functional potency, on the basis of preliminary characterization (24, 25). However, its ultimate mechanism of action and the structural basis for its higher potency remain undetermined.

In the current study, we developed an optimized synthesis of benzoquinazolinone 12, report the first comprehensive pharmacological characterization of its allosteric properties, and use site-directed mutagenesis of specific M_1 mAChR amino acid residues to determine ligand-receptor interactions that govern the actions of this compound at the M_1 mAChR and explain its improved allosteric properties in comparison to BQCA. We also contextualize our experimental findings using molecular modeling and find that many of the key residues that form the allosteric binding pocket at the M_1 mAChR are structurally conserved in other mAChR subtypes (9, 13–15) and even other GPCRs (26, 27). Collectively, our results highlight how allosteric selectivity can be attained not only via selective affinity for a defined binding pocket but also by differential cooperativity between subtypes and can provide the basis for the design of novel M_1 mAChR-selective allosteric ligands.

EXPERIMENTAL PROCEDURES

Materials—CHO FlpIn cells and DMEM were purchased from Invitrogen. FBS was purchased from ThermoTrace (Melbourne, Australia). Hygromycin-B was purchased from Roche. [^{3}H]*N*-methylscopolamine ([^{3}H]NMS); specific activity, 84.1 Ci/mmol) and MicroScint scintillation liquid were purchased from PerkinElmer Life Sciences. IP-One assay kit and reagents were purchased from Cisbio (Codolet, France). All other chemicals were purchased from Sigma-Aldrich. BQCA and benzoquinazolinone 12 were synthesized in house as described in the supplemental materials.

Cell Culture and Receptor Mutagenesis—Mutations of the c-myc-hM_1 mAChR sequence were generated using the QuikChange site-directed mutagenesis kit (Agilent Technologies, La Jolla, CA) following the manufacturer's instructions. All mutations were confirmed by DNA sequencing (Australian Genome Research Facility, Melbourne, Australia). Mutant c-myc-hM_1 mAChR DNA constructs were transfected into FlpIn CHO cells (Invitrogen) and selected using 0.2 mg/ml hygromycin for stable expression.

Whole Cell Radioligand Binding Assays—Saturation binding assays were performed using cells plated at 10^4 cells per well in 96-well Isoplates (PerkinElmer Life Sciences). The following day, the cells were incubated with the orthosteric antagonist [^{3}H]NMS in a final volume of 100 μl of HEPES buffer (10 mM HEPES, 145 mM NaCl, 1 mM $MgSO_4 \cdot 7H_2O$, 10 mM glucose, 5 mM KCl, 2 mM $CaCl_2$, 1.5 mM $NaHCO_3$, pH 7.4) for 2 h at room temperature. For competition binding assays, cells were plated at 2.5×10^4 cells/well. The following day, cells were incubated in a final volume of 100 μl of HEPES buffer containing increasing concentrations of the competing cold ligand ACh (in the absence or presence of increasing concentrations of the allosteric modulator) in a humidified incubator for 1.5 h at 37 °C in the presence of 0.3 nM [^{3}H]NMS. Nonspecific binding was defined in the presence of 100 μM atropine. For all experiments, termination of the assay was performed by rapid removal of radioligand followed by two 100-μl washes with ice-cold 0.9% NaCl buffer. Radioactivity was determined by addition of 100 μl of Microscint scintillation liquid (PerkinElmer Life Sciences) to each well and counting in a MicroBeta plate reader (PerkinElmer Life Sciences).

IP-One Accumulation Assays—The IP-One assay kit (Cisbio, France) was used for the direct quantitative measurement of *myo*-inositol 1 phosphate (IP_1) in FlpIn CHO cells stably expressing either WT or mutant hM_1 mAChRs. Cells were seeded into 384-well Proxy plates (PerkinElmer Life Sciences) at 7,500 cells/well. The following day cells were stimulated with ACh in IP_1 stimulation buffer (10 mM HEPES, 1 mM $CaCl_2$, 0.5 mM $MgCl_2$, 4.2 mM KCl, 146 mM NaCl, 5.5 mM glucose, 50 mM LiCl, pH 7.4) in the absence or presence of increasing concentrations of the allosteric modulator and incubated for 1 h at 37 °C, 5% CO_2. Cells were lysed by the addition of homogenous time resolved FRET reagents, the cryptate-labeled anti-IP_1 antibody, and the d_2-labeled IP_1 analogue, followed by incuba-

tion for 1 h at room temperature. The emission signals were measured at 590 and 665 nm after excitation at 340 nm using the Envision multilabel plate reader (PerkinElmer Life Sciences), and the signal was expressed as the homogenous time resolved FRET ratio: $F = ((\text{fluorescence}_{665\text{ nm}}/\text{fluorescence}_{590\text{ nm}}) \times 10^4)$. Experiments using WT M_1 mAChR CHO FlpIn cells were performed in parallel each day.

Computational Methods for the Model of the Ligand-Receptor Complex—Our previously described hM_1 mAChR model was used for the structural study (10). Docking of the ligands was performed using MOE (Molecular Operating Environment Chemical Computing Group). ACh was docked manually into the receptor model with the quaternized nitrogen of the choline head group interacting with $Asp^{3.32}$ and the ester group situated toward TMIII–TMVI, resembling the position of the ligands described in the mAChR crystal structures (Protein Data Bank codes 3UON (28) and 4DAJ (29)). Benzoquinazolinone 12 was docked into the hM_1 mAChR allosteric binding site described for BQCA. The complex was subjected to an energy minimization using MMFF94X force field and was further refined by means of MD simulations (performed with NAMD2.9 (30) package) using a previously described protocol (31).

Data Analysis—All data were analyzed using Prism 6.01 (GraphPad Software, San Diego, CA). Inhibition binding curves between [^{3}H]NMS and unlabeled ligands were fitted to a one-site binding model (32). Binding interaction studies with allosteric ligands were fitted to the following allosteric ternary complex model (33),

$$Y = \frac{B_{\max}[A]}{[A] + \left(\frac{K_A K_B}{\alpha'[B] + K_B}\right)\left(1 + \frac{[I]}{K_I} + \frac{[B]}{K_B} + \frac{\alpha[I][B]}{K_I K_B}\right)} \quad \text{(Eq. 1)}$$

where Y is the percentage (vehicle control) binding, $B_{\max}$ is the total number of receptors; [A], [B], and [I] are the concentrations of radioligand, allosteric modulator, and the orthosteric ligand, respectively; and K_A, K_B, and K_I are the equilibrium dissociation constants of the radioligand, allosteric modulator, and orthosteric ligand, respectively. α' and α are the binding cooperativities between the allosteric modulator and radioligand and the allosteric ligand and orthosteric ligand, respectively. Values of α (or α') that are >1 denote positive cooperativity, values of <1 (but >0) denote negative cooperativity, and a value of 1 denotes neutral cooperativity.

Concentration-response curves for the interaction between the allosteric ligand and the orthosteric ligand in the IP-One accumulation assays were globally fitted to the following operational model of allosterism and agonism (34),

$$E = \frac{E_m(\tau_A[A](K_B + \alpha\beta[B]) + \tau_B[B]K_A)^n}{([A]K_B + K_A K_B + [B]K_A + \alpha[A][B])^n + (\tau_A[A](K_B + \alpha\beta[B]) + \tau_B[B]K_A)^n} \quad \text{(Eq. 2)}$$

where E_m is the maximum possible cellular response; [A] and [B] are the concentrations of orthosteric and allosteric ligands, respectively; K_A and K_B are the equilibrium dissociation constant of the orthosteric and allosteric ligands, respectively; τ_A and τ_B are operational measures of orthosteric and allosteric ligand efficacy, respectively, α is the binding cooperativity parameter between the orthosteric and allosteric ligand, and β denotes the magnitude of the allosteric effect of the modulator on the efficacy of the orthosteric agonist. In many instances, the individual model parameters of Equation 2 could not be directly estimated via the nonlinear regression algorithm by analysis of the functional data alone, because of parameter redundancy. To facilitate model convergence, therefore, we fixed the equilibrium dissociation constant of each ligand to that determined from the whole cell binding assays. This practice assumes that the affinity determined in the whole cell binding assays is not significantly different from the "functional" affinity operative at the level of the signaling assay, which may not always be the case (35) and thus may lead to a systematic error in the estimate of the operational efficacy parameter, τ. However, because only a single pathway (IP_1) is being considered, the *relative* differences between τ values remain valid for statistical comparison purposes.

All affinity, potency, and cooperativity values were estimated as logarithms (36), and statistical comparisons between values were by one-way analysis of variance using a Dunnett's multiple comparison post test to determine significant differences between mutant receptors and the WT M_1 mAChR. A value of $p < 0.05$ was considered statistically significant.

RESULTS

Identification of Benzoquinazolinone 12 as a Selective Positive Allosteric Modulator of the M_1 mAChR with Higher Affinity than BQCA—In a patent from Merck (25), a series of aryl methyl benzoquinazolinone compounds were disclosed as selective positive allosteric modulators of the M_1 mAChR. One such compound, 3-((1*S*,2*S*)-2-hydroxycyclohexyl)-6-((6-(1-methyl-1*H*-pyrazol-4-yl)pyridin-3-yl)methyl)benzo[*h*]quinazolin-4(3*H*)-one (referred to herein as benzoquinazolinone 12; Fig. 1*A*), was identified as a potent and selective modulator based on its ability to potentiate a single EC_{20} concentration of ACh in a calcium mobilization assay (25, 37). We developed an optimized synthesis, improving the overall yield (Scheme S1 in the supplemental materials) of this compound, followed by detailed pharmacological characterization. We performed whole cell equilibrium competition binding using the radiolabeled antagonist [^{3}H]NMS to study the interaction between ACh and benzoquinazolinone 12. An allosteric ternary complex model (Equation 1) was applied to the data to obtain estimates of modulator affinity for the M_1 mAChR (pK_B), and its binding cooperativity with ACh (Log α) (Fig. 2 and Table 1). This revealed that compared with the prototypical M_1 mAChR positive allosteric modulator BQCA, benzoquinazolinone 12 displays a greater than 50-fold increase in affinity for the M_1 mAChR (Fig. 1*B*, $K_B = 15\ \mu$M and $K_B = 0.3\ \mu$M, for BQCA and benzoquinazolinone 12, respectively) while maintaining a similar level of positive cooperativity with ACh (Fig. 2*A* and Table 1). Interestingly, the modulator displayed high negative cooperativity with the inverse agonist radioligand, which is also a property shared by BQCA (11). Moreover, we confirmed the absolute subtype selectivity of benzoquinazolinone 12 in bind-

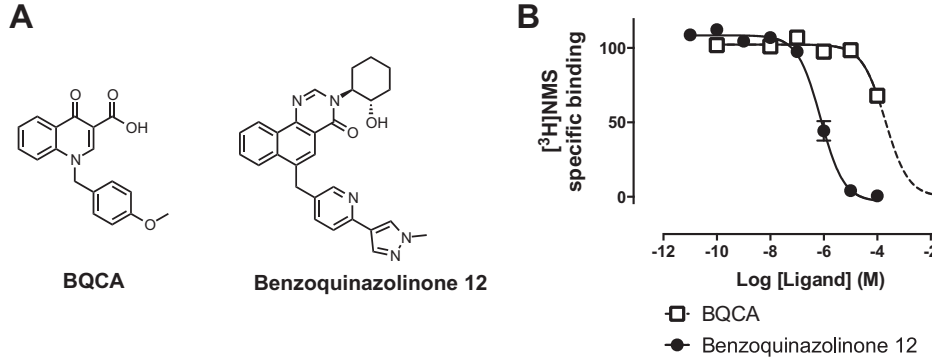

FIGURE 1. *A*, chemical structure of M_1 mAChR-selective positive allosteric modulators. *Left panel*, BQCA. *Right panel*, benzoquinazolinone 12. *B*, BQCA and benzoquinazolinone 12 inhibit the equilibrium binding of [^{3}H]NMS. Data points represent the means ± S.E. of three independent experiments performed in triplicate.

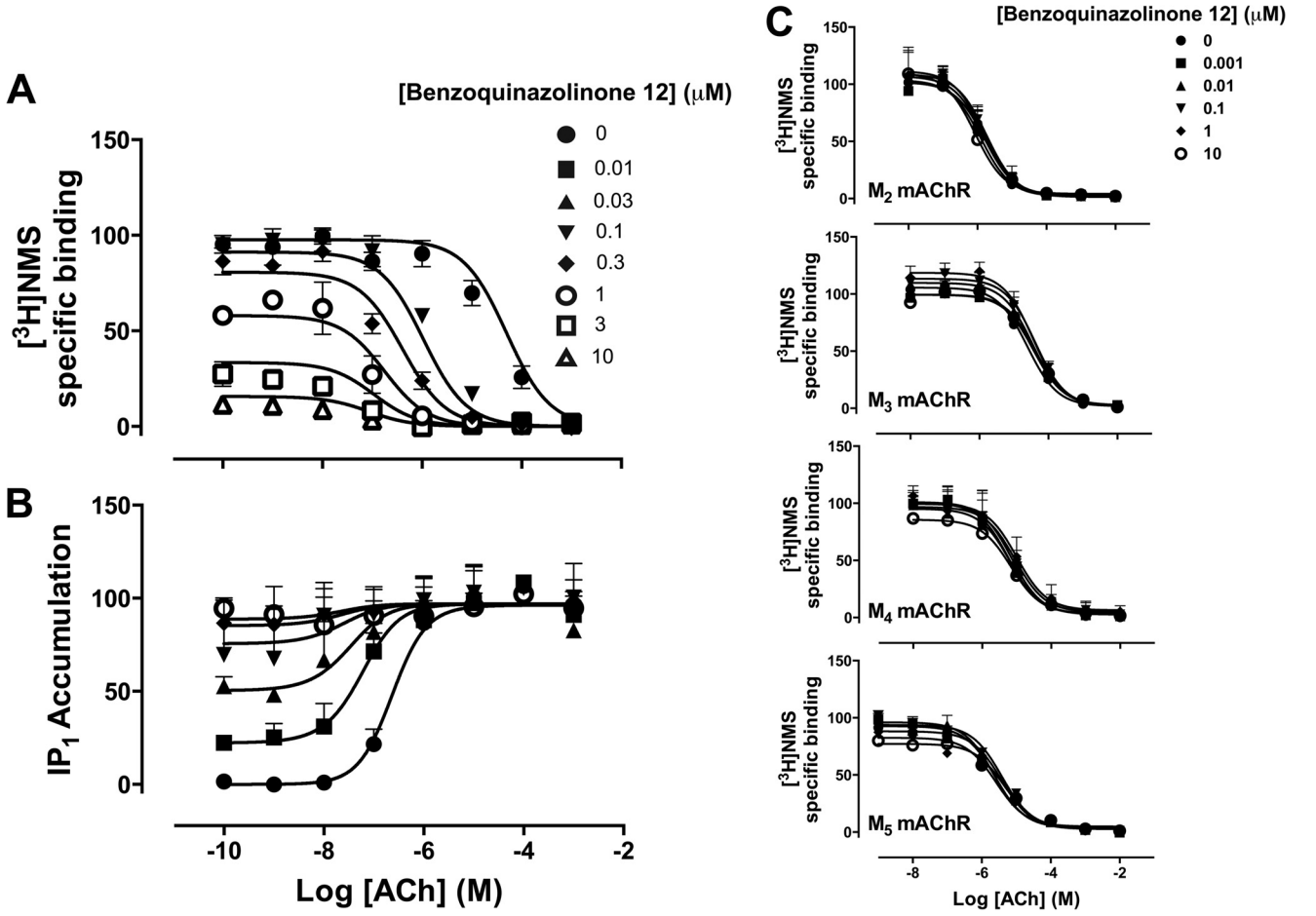

FIGURE 2. **Pharmacological characterization of benzoquinazolinone 12, a high affinity positive allosteric modulator of the M_1 mAChR.** *A*, whole cell radioligand competition binding between [^{3}H]NMS and increasing concentrations of ACh in the absence or presence of increasing concentrations of benzoquinazolinone 12 in CHO FlpIn cells stably expressing WT M_1 mAChR. *B*, interaction between ACh and benzoquinazolinone 12 in an IP_1 accumulation assay in CHO FlpIn cells stably expressing WT M_1 mAChR. *C*, whole cell radioligand competition binding between [^{3}H]NMS and increasing concentrations of ACh in the absence or presence of increasing concentrations of benzoquinazolinone 12 in CHO FlpIn cells stably expressing WT M_{2-5} mAChR. The *curves* in *A* and *C* represent the best fit of an allosteric ternary complex model (Equation 1). The *curves* in *B* represent the best fit of an operational allosteric model (Equation 2).

ing studies using cells expressing the M_2, M_3, M_4, and M_5 mAChRs. As shown in Fig. 2*C*, benzoquinazolinone 12 does not modulate the affinity of ACh at any of these receptor subtypes. We next extended our characterization of this ligand to functional assays. Using IP_1 accumulation as a canonical measure of M_1 mAChR activation resulting from preferential activation of $G\alpha_q$ proteins, and analysis of the data by applying an operational model of allostery (Equation 2), we found that both functional cooperativity (Log $\alpha\beta$) and the intrinsic efficacy (Log τ_B) of benzoquinazolinone 12 were similar to those determined for BQCA (Table 1 and Fig. 2*B*). It was of interest, therefore, to determine the structural basis of the improved allosteric action of benzoquinazolinone 12 as compared with BQCA at the level of receptor residues that this ligand engages and confirm whether benzoquinazolinone 12 engages the same allosteric site as that which we have proposed for BQCA (10).

Effect of Amino Acid Substitution to Ala on the Binding and Function of Benzoquinazolinone 12—As shown above, our pharmacological characterization revealed that benzoquinazolinone 12 displayed a 50-fold increase in allosteric site affinity as compared with BQCA (Table 1). Using a structure-function approach, we next sought to investigate whether benzoquinazolinone 12 binds to the same allosteric pocket as BQCA and the ligand-receptor interactions that govern its binding affinity and cooperativity with ACh.

We focused our investigation on the three amino acid residues we recently identified as contributing to the BQCA binding pocket at the M_1 mAChR (Tyr-$85^{2.64}$ in TM2, Tyr-179 in ECL2, and Trp-$400^{7.35}$ in TM7) (10). In addition, we included Tyr-$82^{2.61}$ in TM2, which is conserved in the related M_2 mAChR and previously identified to contribute to the binding pocket of several allosteric modulators at that subtype (9, 13, 15). Each of these aromatic residues was mutated to Ala, and the mutant M_1 mAChRs were stably expressed in FlpIn CHO cells. Only $W400^{7.35}$A showed >50% reduction in cell surface receptor expression compared with the WT (Table 2). The equilibrium dissociation constants of the orthosteric antagonist [^{3}H]NMS (pK_A) and the orthosteric agonist ACh (pK_I) were significantly reduced at $Y82^{2.61}$A and $Y85^{2.64}$A, whereas only ACh affinity was reduced at $W400^{7.35}$A (Table 2), consistent with previously published findings (13, 14, 38–40).

We then investigated the effect of each of these mutations on the affinity and function of benzoquinazolinone 12. Binding interaction studies revealed that although the affinity of BQCA (pK_B) and its binding cooperativity with ACh (Log α) were not affected by the $Y82^{2.61}$A mutation, benzoquinazolinone 12 displayed a significantly reduced affinity at this mutant receptor with no significant change in its binding cooperativity with ACh (Tables 3 and 4 and Fig. 3, *top* and *middle panels*). Similarly, the pK_B and Log α of BQCA were not affected by the $Y85^{2.64}$A mutation; however, the pK_B (but not the binding cooperativity) of benzoquinazolinone 12 were significantly lower compared with WT. A Tyr in ECL2 (Tyr-179 in the M_1 mAChR) has been found in numerous studies to be involved in the binding of allosteric ligands at the mAChR family (10, 12–15). As shown in Tables 3 and 4 and Fig. 3 (*top* and *middle panels*), mutation of this residue has a profound effect on both BQCA and benzoquinazolinone 12, although mechanistically the effect on BQCA appears to be via reduced cooperativity with ACh, whereas the effect on benzoquinazolinone 12 is a ~100-fold reduction in its affinity for the allosteric site. In contrast, Ala substitution of the conserved Trp-$400^{7.35}$ residue in TM7 completely abolished the binding of both BQCA and benzoquinazolinone 12 (Table 3 and Fig. 3, *top* and *middle panels*), suggesting that this residue is a key direct contributor to the allosteric binding pocket. It is also interesting to note that the binding cooperativity between ACh with benzoquinazolinone 12 was not significantly different from WT at any of the Ala mutants with the exception of $W400^{7.35}$A. As such, these aromatic residues appear to be critical for the binding of benzoquinazolinone 12 but do not participate in the transfer of cooperativity between benzoquinazolinone 12 and the ACh binding site.

Analysis of the allosteric modulator effects at the Ala mutants using an IP_1 accumulation assay revealed that the functional cooperativity (Log $\alpha\beta$) of benzoquinazolinone 12 with ACh is increased at $Y82^{2.61}$A but not affected by Ala substitution at Tyr-$85^{2.64}$ (Table 4 and Fig. 3, *bottom panel*). At both Y179A and $W400^{7.35}$A, BQCA showed no potentiation of ACh. However, in the case of benzoquinazolinone 12 at Y179A,

TABLE 1

Allosteric modulator pharmacological parameters at the WT M_1 mAChR

Estimated parameter values represent the means ± S.E. of three experiments performed in duplicate. pK_B and Log α values were obtained from analysis of the binding interaction data with Equation 1, whereas Log $\alpha\beta$ and Log τ_B values were obtained from analysis of functional interaction data according to Equation 2.

Ligand	pK_B[a]	Log α[b]	Log $\alpha\beta$[c]	Log τ_B[d]
BQCA	4.82 ± 0.09	1.90 ± 0.14	1.54 ± 0.15	0.35 ± 0.07
Benzoquinazolinone 12	6.55 ± 0.03[e]	2.14 ± 0.06	1.79 ± 0.21	0.87 ± 0.20

[a] Negative logarithm of the equilibrium dissociation constant of the modulator
[b] Logarithm of the binding cooperativity factor between the modulator and ACh as estimated by Equation 1; for this analysis, the pK_A of [^{3}H]NMS was constrained to 9.92, and the cooperativity between [^{3}H]NMS with each of the modulators was constrained to −2, consistent with high negative cooperativity between the two ligands.
[c] Logarithm of the functional cooperativity between ACh and the modulator.
[d] Logarithm of the operational efficacy parameter for the modulator.
[e] Significantly different ($p < 0.05$), from BQCA as determined by one-way ANOVA with Dunnett's post hoc test.

TABLE 2

Whole cell equilibrium binding and functional parameters for [^{3}H]NMS and ACh at the WT and mutant M_1 mAChRs

The values represent the means ± S.E. of three experiments performed in duplicate. ND, not determined.

	B_{max}[a]	pK_A[b]	pK_I[c]	pEC_{50}[d]	Log τ_A[e]
M_1 WT	415 ± 15	9.92 ± 0.01	5.11 ± 0.08	6.56 ± 0.11	1.74 ± 0.05
$Y82^{2.61}$A	225 ± 7[f,g]	9.76 ± 0.01[f,g]	4.29 ± 0.07[g]	5.64 ± 0.10[g]	1.02 ± 0.08[g]
$Y85^{2.64}$A	398 ± 10[f]	9.82 ± 0.03[f,g]	4.65 ± 0.06[g]	5.23 ± 0.08[g]	0.57 ± 0.05[g]
Y179A	270 ± 14[f,g]	10.00 ± 0.02[f]	5.05 ± 0.08	5.37 ± 0.12[g]	0.82 ± 0.03[g]
$W400^{7.35}$A	138 ± 6[f,g]	9.95 ± 0.01[f]	4.62 ± 0.08[g]	4.84 ± 0.04[g]	ND
$Y82^{2.61}$F	280 ± 12[g]	10.39 ± 0.01[g]	5.24 ± 0.08	5.59 ± 0.09[g]	0.96 ± 0.06[g]
$Y85^{2.64}$F	295 ± 12[g]	10.04 ± 0.01	4.98 ± 0.09	5.54 ± 0.08[g]	1.09 ± 0.05[g]
Y179F	280 ± 10[g]	9.95 ± 0.07	5.24 ± 0.08	5.68 ± 0.10[g]	0.94 ± 0.08[g]
Y179W	304 ± 8[g]	9.85 ± 0.03	5.08 ± 0.09	5.42 ± 0.09[g]	0.86 ± 0.09[g]
$W400^{7.35}$F	170 ± 12[g]	10.04 ± 0.01	4.82 ± 0.07	5.29 ± 0.09[g]	1.00 ± 0.03[g]
$W400^{7.35}$Y	230 ± 16[g]	10.31 ± 0.05[g]	5.21 ± 0.05	5.86 ± 0.06[g]	1.28 ± 0.06[g]

[a] Maximum density of binding sites per 10^4 cells in counts/min.
[b] Negative logarithm of [^{3}H]NMS equilibrium dissociation constant.
[c] Negative logarithm of ACh equilibrium dissociation constant.
[d] Negative logarithm of the EC_{50} value.
[e] Logarithm of the operational efficacy parameter for ACh as estimated by Equation 2, corrected for changes in receptor expression to allow comparison with WT.
[f] Values taken from the results of Abdul-Ridha *et al.* (10).
[g] Significantly different ($p < 0.05$), from WT value as determined by one-way ANOVA with Dunnett's post hoc test.

TABLE 3

Allosteric modulator equilibrium dissociation constants (pK_B) and binding cooperativity (Log α) estimates for the interaction with ACh at the WT and mutant M_1 mAChRs

Estimated parameter values represent the means ± S.E. of three or four experiments performed in duplicate. pK_B is the negative logarithm of the equilibrium dissociation constant of the modulator, as estimated by Equation 1 from binding interaction studies with ACh; for this analysis, the pK_A of [^{3}H]NMS for the WT and each of the mutants was constrained to the values listed in Table II. The cooperativity between [^{3}H]NMS with each of the modulators was constrained to −2, consistent with high negative cooperativity between the two ligands. ND, not determined (no allosteric modulation).

	pK_B		Log α	
	BQCA	Benzoquinazolinone 12	BQCA	Benzoquinazolinone 12
M_1 WT	4.82 ± 0.06	6.55 ± 0.03	1.90 ± 0.14	2.14 ± 0.06
$Y82^{2.61}A$	4.73 ± 0.06	5.28 ± 0.03[a]	1.96 ± 0.14	2.62 ± 0.15
$Y85^{2.64}A$	4.86 ± 0.08	5.37 ± 0.06[a]	1.53 ± 0.13	2.08 ± 0.11
Y179A	4.68 ± 0.08	4.56 ± 0.19[a]	−0.16 ± 0.28[a]	2.18 ± 0.22
$W400^{7.35}A$	ND	ND	ND	ND
$Y82^{2.61}F$	4.99 ± 0.07	5.67 ± 0.07[a]	1.72 ± 0.14	2.23 ± 0.14
$Y85^{2.64}F$	4.66 ± 0.00	5.86 ± 0.06[a]	1.35 ± 0.15	2.09 ± 0.15
Y179F	4.72 ± 0.07	6.15 ± 0.05[a]	1.88 ± 0.13	2.04 ± 0.13
Y179W	5.06 ± 0.05	6.69 ± 0.04	2.11 ± 0.13	1.78 ± 0.14
$W400^{7.35}F$	4.44 ± 0.08[a]	5.22 ± 0.08[a]	0.83 ± 0.16[a]	2.25 ± 0.15
$W400^{7.35}Y$	4.27 ± 0.10[a]	5.34 ± 0.07[a]	1.50 ± 0.10	2.06 ± 0.14

[a] Significantly different ($p < 0.05$), from WT value as determined by one-way ANOVA with Dunnett's post hoc test.

TABLE 4

Functional cooperativity (Log $\alpha\beta$) estimates for the interaction between the allosteric modulators and ACh at the WT and mutant M_1 mAChRs

Estimated parameter values represent the means ± S.E. of three or four experiments performed in duplicate. Log $\alpha\beta$ is the logarithm of the functional cooperativity factor between the modulator and ACh as estimated by Equation 2. For this analysis, the pK_I values for ACh were fixed to those determined from the radioligand binding assays as listed in Table 2. ND, not determined (no allosteric modulation).

	Log $\alpha\beta$	
	BQCA	Benzoquinazolinone 12
M_1 WT	1.54 ± 0.15	1.79 ± 0.21
$Y82^{2.61}A$	1.93 ± 0.10	2.76 ± 0.27[a]
$Y85^{2.64}A$	1.49 ± 0.04	1.96 ± 0.04
Y179A	ND	1.82 ± 0.14
$W400^{7.35}A$	ND	ND
$Y82^{2.61}F$	1.46 ± 0.20	2.01 ± 0.32
$Y85^{2.64}F$	0.58 ± 0.08[a]	1.82 ± 0.23
Y179F	1.26 ± 0.15	2.15 ± 0.30
Y179W	1.68 ± 0.11	2.53 ± 0.23
$W400^{7.35}F$	0.45 ± 0.07[a]	0.90 ± 0.11
$W400^{7.35}Y$	1.10 ± 0.11	0.57 ± 0.09[a]

[a] Significantly different ($p < 0.05$), from WT value as determined by one-way ANOVA with Dunnett's post hoc test.

potentiation was similar to WT but was abolished at the $W400^{7.35}A$ mutation. The intrinsic efficacy (Log τ_B) of both BQCA and benzoquinazolinone 12 was abolished at each of the M_1 mAChR Ala mutants with the exception of benzoquinazolinone 12 at $Y82^{2.61}A$, where Log τ_B (0.73 ± 0.20) was unchanged relative to WT values (Table 1).

The combined data from the Ala mutation experiments reveal that Tyr-179 in ECL2 and Trp-$400^{7.35}$, residues shown to be of key importance for the activity of BQCA, are also important for the binding of benzoquinazolinone 12. This is consistent with both ligands binding to the same allosteric site within the M_1 mAChR. Furthermore, these results reveal that mutation of Tyr-179 reduces benzoquinazolinone 12 binding affinity but not cooperativity. It is interesting to note that although BQCA was unaffected by both $Y82^{2.61}A$ and $Y85^{2.64}A$ mutations, this was not the case for benzoquinazolinone 12. As such, the replacement of the methoxy group with an aromatic substituent at the 4-position of the benzylic pendant of BQCA or the replacement of the carboxylic acid with the corresponding 3-((1*S*,2*S*)-2-hydroxycyclohexyl) group present in benzoquinazolinone 12 must confer sensitivity to mutation of these TM2 residues.

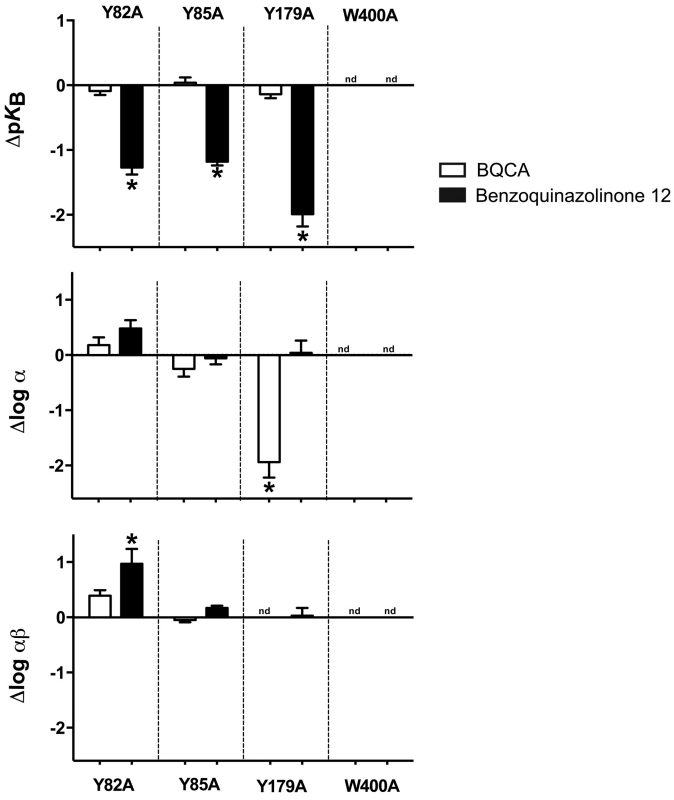

FIGURE 3. **Effect of M_1 mAChR Ala mutations on the binding and function of BQCA and benzoquinazolinone 12.** The *bars* represent the difference for each mutant receptor in allosteric ligand affinity (pK_B, *top panel*), binding cooperativity value (Log α, *middle panel*), or functional cooperativity value (Log $\alpha\beta$, *bottom panel*) of BQCA and benzoquinazolinone 12 relative to WT. The values are derived from interaction experiments in [^{3}H]NMS radioligand binding and IP_1 accumulation (Tables 3 and 4). *, significantly different ($p < 0.05$) from WT as determined by one-way ANOVA with Dunnett's post hoc test. *nd*, not determined (no allosteric modulation).

Molecular Dynamics Simulations and Ligand Docking of Benzoquinazolinone 12 and Comparison with BQCA—To rationalize our findings, we performed ligand docking and molecular dynamic simulations. This resulted in one main pose of benzoquinazolinone 12 in an M_1 mAChR in which ACh was co-bound. This was then compared with the complex of BQCA with carbachol (CCh) bound to the M_1 mAChR obtained using the same methodology in our previous study (10). The complex

for benzoquinazolinone 12 and ACh bound to the modeled M_1 mAChR is shown in Fig. 4. As for CCh in our previous study and analogous to that observed in receptor crystal structure of the M_2 mAChR in complex with the agonist iperoxo (9), Asp-$105^{3.32}$ engages the quaternized choline head group of ACh. Furthermore, ACh lies within a hydrophobic pocket formed by residues Tyr-$106^{3.33}$, Trp-$157^{4.57}$, Tyr-$381^{6.51}$, and Tyr-$408^{7.43}$. In the BQCA-bound complex, stability is added to this binding pocket through a network of hydrogen bond interactions between Tyr-$381^{6.51}$, Tyr-$106^{3.33}$, and Tyr-$404^{7.39}$ (10). These Tyr residues essentially form an aromatic lid over ACh via cation-π interactions. It is interesting to note that in the case of the complex with benzoquinazolinone 12 bound, although the interaction between Tyr-$381^{6.51}$ and Tyr-$106^{3.33}$ is maintained, Tyr-$404^{7.39}$ faces TM2 and interacts with Tyr-$82^{2.61}$ (Fig. 4).

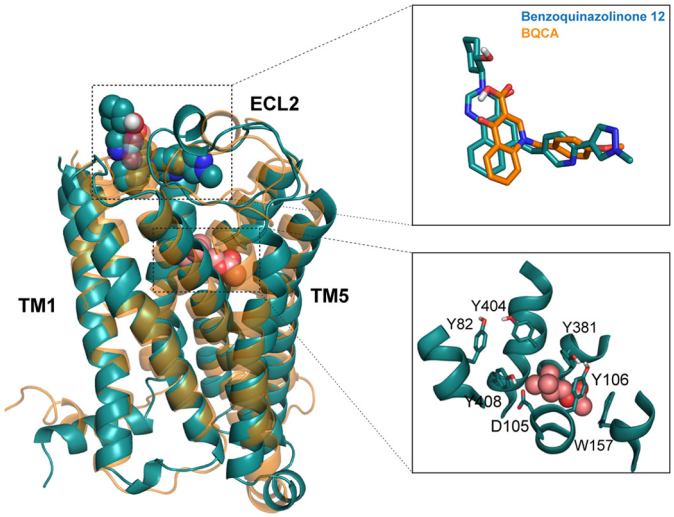

FIGURE 4. **Structural homology model of the M_1 mAChR complex co-bound with CCh-BQCA (*orange*) or ACh-benzoquinazolinone 12 (*blue*).** The overall structure of the BQCA-bound M_1 mAChR model (*orange*) is similar to that of the benzoquinazolinone 12-bound M_1 mAChR model (*blue*). ACh (*pink*), BQCA (*orange*), and benzoquinazolinone 12 (*blue*) are shown as *spheres* colored according to element. *Top inset*, overlay of the BQCA (*orange*) and benzoquinazolinone 12 (*blue*) poses represented as stick structures. *Bottom inset*, ACh binding site in benzoquinazolinone 12-bound M_1 mAChR complex model. Important residues are shown as *sticks*.

Analysis of the molecular dynamics trajectories reveals that both BQCA and benzoquinazolinone 12 adopt a similar pose (Fig. 5). In both cases, the binding site for the ligands is defined by residues from TM2, TM7, and ECL2 and is in agreement with our mutagenesis studies. In particular, the significant effects of the mutation of Tyr-179 to Ala in ECL2 and Trp-$400^{7.35}$ in TM7 on the pharmacology of BQCA and benzoquinazolinone 12 can be reconciled with the poses of each ligand. In both BQCA and benzoquinazolinone 12 complexes, Tyr-179 is predicted to contribute to the stable binding of the compounds via hydrophobic/edge to face π-π interactions with the bicyclic 4-oxoquinoline core of BQCA or tricyclic benzo-[*h*]quinazolin-4(3*H*)-one core of benzoquinazolinone 12. In addition, the hydroxyl group of Tyr-179 may form a polar or potential hydrogen bond interaction with the OH group of the 3-((1*S*,2*S*)-2-hydroxycyclohexyl) moiety of benzoquinazolinone 12. This interaction cannot take place in the BQCA bound complex, because BQCA does not bear the corresponding amide moiety. Trp-$400^{7.35}$ is predicted to interact with the benzylic pendant of both BQCA and benzoquinazolinone 12. However, in the BQCA bound complex, Trp-$400^{7.35}$ is positioned horizontally below the benzylic pendant of BQCA and is predicted to make a π-π stacking interaction with this moiety (Fig. 5*A*). In comparison, to accommodate the additional *N*-methylpyrazole substituent of benzoquinazolinone 12, Trp-$400^{7.35}$ is positioned in a more vertical orientation and extends toward TM6. This orientation allows the following interactions: (*a*) edge to face π-π/hydrophobic interactions with the *N*-methylpyrazole substituent of benzoquinazolinone 12, (*b*) hydrophobic sandwich of pyrazole substituent between Trp-$400^{7.35}$ and Tyr-179, (*c*) a π-π stacking interaction with Phe-182 in ECL2,

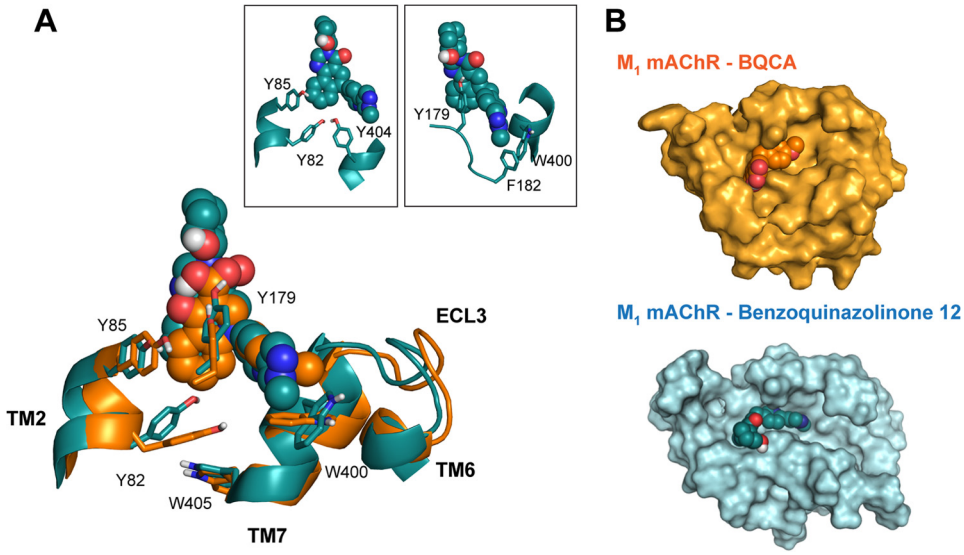

FIGURE 5. **Proposed arrangement of the binding sites of BQCA and benzoquinazolinone 12 at the M_1 mAChR.** *A*, extracellular view of the binding sites of BQCA and benzoquinazolinone 12. BQCA (*orange*) and benzoquinazolinone 12 (*blue*) are shown as *spheres* colored according to element. Important residues are shown as sticks. *Insets*, positions of Tyr-$2^{2.61}$, Tyr-$85^{2.64}$, Tyr-$404^{7.39}$, Tyr-179, Phe-182, and Trp-$400^{7.35}$ in the ACh-benzoquinazolinone 12-bound M_1 mAChR model. *B*, extracellular view of the BQCA-bound (*orange*) and benzoquinazolinone 12-bound (*blue*) M_1 mAChR models showing a tighter pocket for benzoquinazolinone 12 as compared with that predicted for BQCA.

which appears to pull ECL2 toward TM7, creating a tighter allosteric binding pocket as compared with that observed in the BQCA bound complex (Fig. 5, *A* and *B*). The additional interactions observed in the complex with benzoquinazolinone 12 can explain, in part, the increased affinity of benzoquinazolinone 12 as compared with BQCA. The TM2 residues Tyr-85$^{2.64}$ and Tyr-82$^{2.61}$ are predicted to delimit the allosteric site in both complexes via edge to face π-π/hydrophobic interactions with the 4-oxoquinoline ring system in the case of BQCA. However, the tricyclic core of benzoquinazolinone 12 is closer to TM2 (Fig. 5*A*), allowing π interactions with both residues, which may also contribute to the higher binding affinity of benzoquinazolinone 12. In agreement with this pose, mutation of both Tyr-85$^{2.64}$ and Tyr-82$^{2.61}$ caused a greater than 10-fold loss of affinity for benzoquinazolinone 12, whereas no effect upon the affinity of BQCA was observed. The closer interaction of Tyr-82$^{2.61}$ with benzoquinazolinone 12 may allow for increased ligand-receptor hydrophobic interactions that may account for the higher binding affinity of this ligand at the allosteric binding site (Fig. 5, *A* and *B*). Of interest, Tyr-82$^{2.61}$ makes a H-bond interaction with Tyr-404$^{7.39}$, one of the residues that forms the aromatic 'lid' over the CCh binding site in the BQCA bound complex. As such, this interaction may provide part of the cooperative mechanism through which binding of benzoquinazolinone 12 to the allosteric pocket modulates the shape of and ligand receptor interactions within the orthosteric pocket.

Effect of Conservative Amino Acid Substitution on the Binding and Function of BQCA and Benzoquinazolinone 12—Our mutagenesis and modeling studies highlight the particular importance of Tyr-85$^{2.64}$ and Tyr-82$^{2.61}$ in TM2, Tyr-179 in ECL2, and Trp-400$^{7.35}$ in TM7. However, such an Ala scanning approach, although useful to highlight the importance of individual residues for the binding of a ligand, can only give limited information regarding the nature of these interactions. In particular our modeling studies suggested that Tyr-85$^{2.64}$, Tyr-82$^{2.61}$, and Tyr-179 might participate in a hydrogen bond network with the ligand and/or with other residues in the complex with benzoquinazolinone 12 but not in the BQCA complex. To further understand the contribution of each of the aromatic amino acid residues to the allosteric binding pocket, we tested the effects of more subtle amino acid substitutions on ligand binding and function. We mutated each Tyr residue (Tyr-82$^{2.61}$, Tyr-85$^{2.64}$, and Tyr-179) or Trp-400$^{7.35}$ to Phe. In addition, we mutated Tyr-179 to Trp with the expectation that this larger, bicyclic aromatic residue would be able to make stronger interactions with the benzylic pendant of both ligands as suggested from our BQCA analogues SAR data (41), Ala mutation data, and modeling results. We compared the effects of these mutations upon the pharmacology of both BQCA and benzoquinazolinone 12 (Fig. 6).

As with the Ala substitutions, we first tested the effects of the mutants on orthosteric ligand binding and cell surface receptor expression. Whole cell [^{3}H]NMS saturation binding experiments showed that all the mutations led to a significant reduction in cell surface receptor expression compared with the WT (Table 2). The maximum decrease in receptor expression relative to WT was ~2-fold at Trp-400$^{7.35}$F. In addition to receptor expression, the equilibrium dissociation constant of the

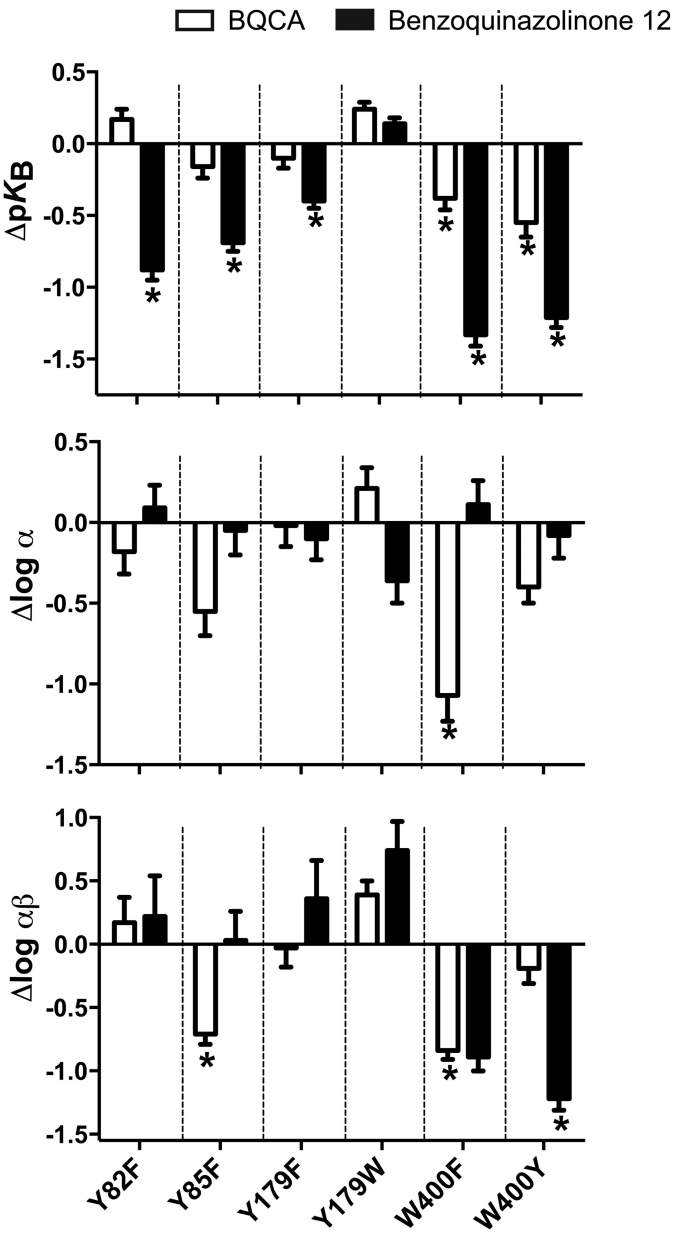

FIGURE 6. **Effect of M_1 mAChR conservative mutations on the binding and function of BQCA and benzoquinazolinone 12.** The *bars* represent the difference for each mutant receptor in allosteric ligand affinity (pK_B, *top panel*), binding cooperativity value (Log α, *middle panel*), or functional cooperativity value (Log $\alpha\beta$, *bottom panel*) of BQCA and benzoquinazolinone 12 relative to WT. The values are derived from interaction experiments in [^{3}H]NMS radioligand binding and IP_1 accumulation (Tables 3 and 4). *, significantly different ($p < 0.05$) from WT as determined by one-way ANOVA with Dunnett's post hoc test.

orthosteric antagonist [^{3}H]NMS (pK_A) or the orthosteric agonist ACh (pK_I) were also determined (Table 2). Y82$^{2.61}$F and W400$^{7.35}$Y caused slight but significant increases in [^{3}H]NMS affinity. The remaining mutants had no effect on orthosteric ligand binding. The potency (EC_{50}) of ACh in IP_1 assays was significantly reduced at all the mutants, likely because of the reduction in receptor surface expression (Table 2).

To determine the effects of each mutant on allosteric ligand binding affinity (pK_B) and cooperativity (Log α) with ACh, we performed whole cell binding interaction studies for both BQCA and benzoquinazolinone 12. The pK_B and Log α of

BQCA were unchanged at the Tyr to Phe mutants (Y85$^{2.64}$F, Y82$^{2.61}$F, and Y179F) (Table 3), suggesting that the ability of these residues to make hydrophobic, rather than polar, interactions is predominant for their role in BQCA binding and function. In contrast, substitution of the conserved aromatic residue Trp-400 to less bulky aromatic amino acids (W400$^{7.35}$F and W400$^{7.35}$Y) caused significant reductions in BQCA and benzoquinazolinone 12 binding affinity (Table 3). Interestingly, substitution of Tyr-85$^{2.64}$ and Tyr-82$^{2.61}$ in TM2 and Tyr-179 in ECL2 to Phe resulted in significant decreases in the binding affinity of benzoquinazolinone 12. This suggests that the ability to make polar interactions has a significant contribution to their role in the binding of benzoquinazolinone 12 and is in agreement with the network of interactions predicted by our modeling experiments. Replacement of Tyr-179 with a Trp did not significantly change the affinity of either BQCA or benzoquinazolinone 12. The binding cooperativity of BQCA with ACh was only reduced at W400$^{7.35}$F (Table 3). Interestingly, and in agreement with the results at the corresponding Ala mutants, the binding cooperativity of benzoquinazolinone 12 with ACh was not significantly changed at any of these conservative mutants (Table 3).

We extended our study to look at the effect of these mutations upon the action of BQCA and benzoquinazolinone 12 in a functional assay. Analysis of the allosteric potentiation of ACh by BQCA in an IP_1 accumulation assay revealed that the functional cooperativity was profoundly reduced at Y85$^{2.64}$F and W400$^{7.35}$F, although benzoquinazolinone 12 showed reduced cooperativity with ACh at W400$^{7.35}$Y but not the other mutations. Both ligands showed unchanged cooperativity at Y179W (Table 4), in agreement with the binding results.

DISCUSSION

Significant efforts have been directed at the discovery of novel selective ligands of the M_1 mAChR as a therapeutic approach for neurocognitive disorders, such as Alzheimer's disease (3, 42). From these efforts, the compounds that display the most exquisite selectivity target an allosteric site of this receptor, as exemplified by BQCA (6, 12). More recently, benzoquinazolinone 12, an analogue of BQCA, was described as a modulator with improved allosteric activity (25). We have now provided a detailed characterization of benzoquinazolinone 12, demonstrating that its increase in activity at the M_1 mAChR as compared with BQCA is largely derived from an approximately 50-fold increase in affinity, whereas both functional and binding cooperativity with ACh are not substantially changed. Furthermore, benzoquinazolinone 12 not only displays high positive cooperativity with agonist binding but also high negative cooperativity with the binding of the orthosteric antagonist [^{3}H]NMS. Thus, benzoquinazolinone 12 appears to conform to the classic Monod-Wyman-Changeux mechanism of action previously described for BQCA (11).

Our previous SAR study of derivatives of BQCA revealed four discrete areas of structural modification that conferred distinct effects on the allosteric activity of these compounds (41). Alternative substitution of the 5- and 8-positions of the quinolone ring appeared to modulate intrinsic efficacy (τ_B); isosteric replacement of the carboxylic acid moiety or amide derivatives modulated cooperativity parameters (α and β) and, finally, replacement of the pendant *N*-alkyl group modulated affinity (pK_B). The ability to enrich allosteric SAR by dissecting these molecular parameters can also be used to link these parameters to receptor structural information, thus yielding new insights into the structural basis of allostery. In the current study, we applied this approach to explore the structural basis of the improved allosteric activity of benzoquinazolinone 12 at the M_1 mAChR in comparison to BQCA. This is important, because the location and nature of the allosteric site for most GPCRs remains poorly characterized. Our combined mutagenesis and molecular modeling experiments provide evidence that BQCA and benzoquinazolinone 12 occupy a similar pocket of the M_1 mAChR. In our previous study, we proposed that Tyr-179 (in ECL2) and Trp-400$^{7.35}$ were of key importance for the activity of BQCA (10). In the current work, we confirmed this result and found that the W400$^{7.35}$A mutation abrogated detectable binding of compound benzoquinazolinone 12, whereas the compound also displayed a 100-fold decrease in affinity at the Y179A mutant. However, this latter mutation had no effect upon the cooperativity of benzoquinazolinone 12. In agreement with the role of Tyr-179 as a determinant of both BQCA and benzoquinazolinone 12 affinity or transmission of cooperativity, our modeling studies reveal that this residue provides hydrophobic/edge to face π-π interactions with the bicyclic core of BQCA or tricyclic core of benzoquinazolinone 12, although the rotameric orientation of the residue differs slightly depending on the molecule bound. Indeed, mutation of this Tyr to the aromatic residues Phe or Trp had no effect, confirming that Tyr-179 makes predominantly hydrophobic interactions with both ligands. Trp-400$^{7.35}$ is predicted to interact with the benzylic pendant of both BQCA and benzoquinazolinone 12. Indeed, the importance of this interaction is validated both by our structure-function analysis and by the SAR of BQCA derivatives (41) and benzoquinazolinone 12. The mutation of Trp-400$^{7.35}$ to Ala completely abolished detectable binding of all allosteric modulators in this study. Furthermore, the additional aromatic substitution of the 4-position of the benzylic pendant conferred a gain in affinity. Such substitutions would enhance the ability of these ligands to make hydrophobic interactions with Trp-400$^{7.35}$. In agreement with this hypothesis, the conservative mutation of Trp-400$^{7.35}$ to the smaller Phe or Tyr conferred decreases in affinity. In the BQCA-bound complex Trp-400$^{7.35}$ is positioned horizontally below the benzylic pendant of BQCA and makes a π-π stacking interaction with this moiety. In comparison, to accommodate the additional pyrazole substituent of benzoquinazolinone 12, Trp-400$^{7.35}$ is positioned in a more vertical orientation and extends toward TM6. This change in orientation allows the pyrazole substituent of benzoquinazolinone 12 to make hydrophobic interactions with both Trp-400$^{7.35}$ and Tyr-179. Of interest, in the M_2 mAChR crystal structure, Trp-422$^{7.35}$ adopts a vertical conformation in the presence of the positive allosteric modulator LY2119620 and a horizontal conformation with iperoxo alone. The vertical conformation of this residue in the M_2-iperoxo-LY2119620 complex allows it to engage in an aromatic stacking interaction with the modulator (9).

The TM2 residues Tyr-85$^{2.64}$ and Tyr-82$^{2.61}$ are predicted to line the allosteric pocket in both BQCA and benzoquinazolinone 12-bound complexes. However, the tricyclic core of benzoquinazolinone 12 is predicted to be closer to TM2, conferring stronger interactions with both residues, which may contribute to the higher binding affinity of benzoquinazolinone 12. In agreement with this pose, mutation of both Tyr-85$^{2.64}$ and Tyr-82$^{2.61}$ to Ala caused a greater than 10-fold loss of affinity for benzoquinazolinone 12, whereas no effect upon the affinity of BQCA was observed. Tyr-82$^{2.61}$ was predicted to make a H-bond interaction with Tyr-404$^{7.39}$ in the benzoquinazolinone 12-bound complex but not in the BQCA-bound complex. Interestingly, mutation of Tyr-82$^{2.61}$ to Phe caused a significant decrease in the pK_B of benzoquinazolinone 12 for the mutant receptor but not BQCA. Tyr$^{7.39}$ has been shown to play a key role in the binding of the orthosteric ligand iperoxo in the active structure of the M_2 mAChR, forming an aromatic lid over the ligand amine, an interaction present in our BQCA bound complex. Indeed, this residue has been shown to play an important role in orthosteric ligand binding at a number of GPCRs. Of interest, mutation of the corresponding residue in the M_4 mAChR caused a significant decrease in the binding cooperativity of the positive allosteric modulator LY2033298 with ACh (14). This suggests that this residue is also important for transfer of cooperativity between the allosteric and orthosteric binding sites. It is also interesting to note that the additional pyrimidinone ring in benzoquinazolinone 12 is predicted to be positioned above the allosteric binding pocket. Although the functional significance of this portion of the modulator has not yet been investigated through structure-activity relationships, a recent report by Kuduk *et al.* (44) highlights the importance of the intramolecular hydrogen bond between the 4-oxo moiety and 3-carboxylic acid group present in bicyclic BQCA-type scaffolds, suggesting that this hydrogen bond is key for allosteric activity. We hypothesize that the pyrimidinone ring that forms part of the tricyclic core in benzoquinazolinone 12 formalizes the rigidity imparted by this intramolecular hydrogen bond.

Dror *et al.* (13) recently used molecular dynamics to identify two binding centers in the extra cellular vestibule of the M_2 mAChR that are implicated in the binding of several structurally diverse positive and negative allosteric modulators, each of the binding centers is defined by a pair of aromatic residues (Centre 1 Tyr-177^{ECL2} and Trp$^{7.35}$, Centre 2 Tyr$^{2.61}$, and Tyr$^{2.64}$). Additionally, the M_2 mAChR crystal structure co-bound by the orthosteric agonist iperoxo and the positive allosteric modulator LY2119620 shows that the aromatic rings of the modulator are situated directly between Tyr-177 in ECL2 and Trp-422$^{7.35}$, forming a three-layered aromatic stack (9). A previous mutagenesis study implicated Tyr-177 as a contact for the LY2119620 congener LY2033298 at the M_2 mAChRs (43). We identified the equivalent M_1 mAChR residues as key contributors for the binding and function of BQCA (10) and benzoquinazolinone 12. In particular, because benzoquinazolinone 12 displays significantly higher affinity than BQCA, we were able to demonstrate that Tyr-179 has a major role in the binding of allosteric ligands or in the transfer of cooperativity. Tyr$^{2.64}$ and Trp$^{7.35}$ are conserved across all mAChR receptor subtypes, Tyr$^{2.61}$ is conserved across all but the M_3 mAChR (where it is a similarly aromatic Phe residue), and Tyr-179 is only present at the M_1 and M_2 mAChRs but is a Phe at the M_3 and M_4 mAChRs. This is consistent with BQCA and its analogues sharing a common binding site with other prototypical mAChR allosteric modulators. Although these findings provide insight into the location of the binding pocket for mAChR allosteric modulators, they do not explain how some of these ligands achieve subtype selectivity. As we hypothesized in our earlier studies, it is likely that receptor subtype selectivity is achieved via selective cooperativity of the modulators with the orthosteric ligands.

In summary, our combined mutagenesis and molecular dynamics simulations have validated the allosteric binding pocket we previously described for BQCA and provided a mechanistic basis for observed SAR of M_1 mAChR positive allosteric modulators. In particular, we have demonstrated that benzoquinazolinone 12 displays a significant increase in affinity at the M_1 mAChR and identified the ligand-receptor interactions that confer this increase. These insights will provide the basis for the development of novel M_1 mAChR selective allosteric ligands that explore new chemical space.

Acknowledgment—We are grateful to Dr. Ann Stewart for technical assistance.

REFERENCES

1. Katritch, V., Cherezov, V., and Stevens, R. C. (2013) Structure-function of the G protein-coupled receptor superfamily. *Annu. Rev. Pharmacol. Toxicol.* **53,** 531–556
2. Kruse, A. C., Hu, J., Kobilka, B. K., and Wess, J. (2014) Muscarinic acetylcholine receptor X-ray structures: potential implications for drug development. *Curr. Opin. Pharmacol.* **16,** 24–30
3. Conn, P. J., Christopoulos, A., and Lindsley, C. W. (2009) Allosteric modulators of GPCRs: a novel approach for the treatment of CNS disorders. *Nat. Rev. Drug Discov.* **8,** 41–54
4. Jones, C. K., Byun, N., and Bubser, M. (2012) Muscarinic and nicotinic acetylcholine receptor agonists and allosteric modulators for the treatment of schizophrenia. *Neuropsychopharmacology* **37,** 16–42
5. Byun, N. E., Grannan, M., Bubser, M., Barry, R. L., Thompson, A., Rosanelli, J., Gowrishankar, R., Kelm, N. D., Damon, S., Bridges, T. M., Melancon, B. J., Tarr, J. C., Brogan, J. T., Avison, M. J., Deutch, A. Y., Wess, J., Wood, M. R., Lindsley, C. W., Gore, J. C., Conn, P. J., and Jones, C. K. (2014) Antipsychotic drug-like effects of the selective M4 muscarinic acetylcholine receptor positive allosteric modulator VU0152100. *Neuropsychopharmacology* **39,** 1578–1593
6. Shirey, J. K., Brady, A. E., Jones, P. J., Davis, A. A., Bridges, T. M., Kennedy, J. P., Jadhav, S. B., Menon, U. N., Xiang, Z., Watson, M. L., Christian, E. P., Doherty, J. J., Quirk, M. C., Snyder, D. H., Lah, J. J., Levey, A. I., Nicolle, M. M., Lindsley, C. W., and Conn, P. J. (2009) A selective allosteric potentiator of the M1 muscarinic acetylcholine receptor increases activity of medial prefrontal cortical neurons and restores impairments in reversal learning. *J. Neurosci.* **29,** 14271–14286
7. Stevens, R. C., Cherezov, V., Katritch, V., Abagyan, R., Kuhn, P., Rosen, H., and Wüthrich, K. (2013) The GPCR Network: a large-scale collaboration to determine human GPCR structure and function. *Nat. Rev. Drug Discov.* **12,** 25–34
8. Venkatakrishnan, A. J., Deupi, X., Lebon, G., Tate, C. G., Schertler, G. F., and Babu, M. M. (2013) Molecular signatures of G-protein-coupled receptors. *Nature* **494,** 185–194
9. Kruse, A. C., Ring, A. M., Manglik, A., Hu, J., Hu, K., Eitel, K., Hübner, H., Pardon, E., Valant, C., Sexton, P. M., Christopoulos, A., Felder, C. C., Gmeiner, P., Steyaert, J., Weis, W. I., Garcia, K. C., Wess, J., and Kobilka, B. K. (2013) Activation and allosteric modulation of a muscarinic acetylcholine receptor. *Nature* **504,** 101–106
10. Abdul-Ridha, A., López, L., Keov, P., Thal, D. M., Mistry, S. N., Sexton,

P. M., Lane, J. R., Canals, M., and Christopoulos, A. (2014) Molecular determinants of allosteric modulation at the M1 muscarinic acetylcholine receptor. *J. Biol. Chem.* **289,** 6067–6079
11. Canals, M., Lane, J. R., Wen, A., Scammells, P. J., Sexton, P. M., and Christopoulos, A. (2012) A Monod-Wyman-Changeux mechanism can explain G protein-coupled receptor (GPCR) allosteric modulation. *J. Biol. Chem.* **287,** 650–659
12. Ma, L., Seager, M. A., Wittmann, M., Jacobson, M., Bickel, D., Burno, M., Jones, K., Graufelds, V. K., Xu, G., Pearson, M., McCampbell, A., Gaspar, R., Shughrue, P., Danziger, A., Regan, C., Flick, R., Pascarella, D., Garson, S., Doran, S., Kreatsoulas, C., Veng, L., Lindsley, C. W., Shipe, W., Kuduk, S., Sur, C., Kinney, G., Seabrook, G. R., and Ray, W. J. (2009) Selective activation of the M1 muscarinic acetylcholine receptor achieved by allosteric potentiation. *Proc. Natl. Acad. Sci. U.S.A.* **106,** 15950–15955
13. Dror, R. O., Green, H. F., Valant, C., Borhani, D. W., Valcourt, J. R., Pan, A. C., Arlow, D. H., Canals, M., Lane, J. R., Rahmani, R., Baell, J. B., Sexton, P. M., Christopoulos, A., and Shaw, D. E. (2013) Structural basis for modulation of a G-protein-coupled receptor by allosteric drugs. *Nature* **503,** 295–299
14. Nawaratne, V., Leach, K., Felder, C. C., Sexton, P. M., and Christopoulos, A. (2010) Structural determinants of allosteric agonism and modulation at the M4 muscarinic acetylcholine receptor: identification of ligand-specific and global activation mechanisms. *J. Biol. Chem.* **285,** 19012–19021
15. May, L. T., Avlani, V. A., Langmead, C. J., Herdon, H. J., Wood, M. D., Sexton, P. M., and Christopoulos, A. (2007) Structure-function studies of allosteric agonism at M2 muscarinic acetylcholine receptors. *Mol. Pharmacol.* **72,** 463–476
16. Matsui, H., Lazareno, S., and Birdsall, N. J. (1995) Probing of the location of the allosteric site on m1 muscarinic receptors by site-directed mutagenesis. *Mol. Pharmacol.* **47,** 88–98
17. Lazareno, S., Dolezal, V., Popham, A., and Birdsall, N. J. (2004) Thiochrome enhances acetylcholine affinity at muscarinic M4 receptors: receptor subtype selectivity via cooperativity rather than affinity. *Mol. Pharmacol.* **65,** 257–266
18. Lebois, E. P., Bridges, T. M., Lewis, L. M., Dawson, E. S., Kane, A. S., Xiang, Z., Jadhav, S. B., Yin, H., Kennedy, J. P., Meiler, J., Niswender, C. M., Jones, C. K., Conn, P. J., Weaver, C. D., and Lindsley, C. W. (2010) Discovery and characterization of novel subtype-selective allosteric agonists for the investigation of M_1 receptor function in the central nervous system. *ACS Chem. Neurosci.* **1,** 104–121
19. Melancon, B. J., Tarr, J. C., Panarese, J. D., Wood, M. R., and Lindsley, C. W. (2013) Allosteric modulation of the M1 muscarinic acetylcholine receptor: improving cognition and a potential treatment for schizophrenia and Alzheimer's disease. *Drug Discovery Today* **18,** 1185–1199
20. Tarr, J. C., Turlington, M. L., Reid, P. R., Utley, T. J., Sheffler, D. J., Cho, H. P., Klar, R., Pancani, T., Klein, M. T., Bridges, T. M., Morrison, R. D., Blobaum, A. L., Xiang, Z., Daniels, J. S., Niswender, C. M., Conn, P. J., Wood, M. R., and Lindsley, C. W. (2012) Targeting selective activation of M1 for the treatment of Alzheimer's disease: further chemical optimization and pharmacological characterization of the M1 positive allosteric modulator ML169. *ACS Chem. Neurosci.* **3,** 884–895
21. Foster, D. J., Choi, D. L., Conn, P. J., and Rook, J. M. (2014) Activation of M1 and M4 muscarinic receptors as potential treatments for Alzheimer's disease and schizophrenia. *Neuropsychiatr. Dis. Treat.* **10,** 183–191
22. Nickols, H. H., and Conn, P. J. (2014) Development of allosteric modulators of GPCRs for treatment of CNS disorders. *Neurobiol. Dis.* **61,** 55–71
23. Nathan, P. J., Watson, J., Lund, J., Davies, C. H., Peters, G., Dodds, C. M., Swirski, B., Lawrence, P., Bentley, G. D., O'Neill, B. V., Robertson, J., Watson, S., Jones, G. A., Maruff, P., Croft, R. J., Laruelle, M., and Bullmore, E. T. (2013) The potent M1 receptor allosteric agonist GSK1034702 improves episodic memory in humans in the nicotine abstinence model of cognitive dysfunction. *Int. J. Neuropsychopharmacol.* **16,** 721–731
24. Kuduk, S. D., and Beshore, D. C. (2012) Novel M1 allosteric ligands: a patent review. *Expert. Opin. Ther. Pat.* **22,** 1385–1398
25. Kuduk, S. D., Beshore, D. C., DiMarco, C. N., and Greshock, T. J. (May 27, 2010) U. S. Patent WO 2010/059773
26. Kennedy, D. P., McRobb, F. M., Leonhardt, S. A., Purdy, M., Figler, H., Marshall, M. A., Chordia, M., Figler, R., Linden, J., Abagyan, R., and Yeager, M. (2014) The second extracellular loop of the adenosine A1 receptor mediates activity of allosteric enhancers. *Mol. Pharmacol.* **85,** 301–309
27. Ragnarsson, L., Wang, C. I., Andersson, A., Fajarningsih, D., Monks, T., Brust, A., Rosengren, K. J., and Lewis, R. J. (2013) Conopeptide rho-TIA defines a new allosteric site on the extracellular surface of the α1B-adrenoceptor. *J. Biol. Chem.* **288,** 1814–1827
28. Haga, K., Kruse, A. C., Asada, H., Yurugi-Kobayashi, T., Shiroishi, M., Zhang, C., Weis, W. I., Okada, T., Kobilka, B. K., Haga, T., and Kobayashi, T. (2012) Structure of the human M2 muscarinic acetylcholine receptor bound to an antagonist. *Nature* **482,** 547–551
29. Kruse, A. C., Hu, J., Pan, A. C., Arlow, D. H., Rosenbaum, D. M., Rosemond, E., Green, H. F., Liu, T., Chae, P. S., Dror, R. O., Shaw, D. E., Weis, W. I., Wess, J., and Kobilka, B. K. (2012) Structure and dynamics of the M3 muscarinic acetylcholine receptor. *Nature* **482,** 552–556
30. Phillips, J. C., Braun, R., Wang, W., Gumbart, J., Tajkhorshid, E., Villa, E., Chipot, C., Skeel, R. D., Kalé, L., and Schulten, K. (2005) Scalable molecular dynamics with NAMD. *J. Comput. Chem.* **26,** 1781–1802
31. Shonberg, J., Herenbrink, C. K., López, L., Christopoulos, A., Scammells, P. J., Capuano, B., and Lane, J. R. (2013) A structure-activity analysis of biased agonism at the dopamine D2 receptor. *J. Med. Chem.* **56,** 9199–9221
32. Motulsky H, C. A. (2004) *Fitting Models to Biological Data Using Linear and Nonlinear Regression: A Practical Guide to Curve Fitting*, Oxford University Press, New York
33. Leach, K., Loiacono, R. E., Felder, C. C., McKinzie, D. L., Mogg, A., Shaw, D. B., Sexton, P. M., and Christopoulos, A. (2010) Molecular mechanisms of action and in vivo validation of an M4 muscarinic acetylcholine receptor allosteric modulator with potential antipsychotic properties. *Neuropsychopharmacology* **35,** 855–869
34. Leach, K., Sexton, P. M., and Christopoulos, A. (2007) Allosteric GPCR modulators: taking advantage of permissive receptor pharmacology. *Trends Pharmacol. Sci.* **28,** 382–389
35. Kenakin, T., and Christopoulos, A. (2013) Signalling bias in new drug discovery: detection, quantification and therapeutic impact. *Nat. Rev. Drug Discov.* **12,** 205–216
36. Christopoulos, A. (1998) Assessing the distribution of parameters in models of ligand-receptor interaction: to log or not to log. *Trends Pharmacol. Sci.* **19,** 351–357
37. Kuduk, S. D., Chang, R. K., Di Marco, C. N., Ray, W. J., Ma, L., Wittmann, M., Seager, M. A., Koeplinger, K. A., Thompson, C. D., Hartman, G. D., and Bilodeau, M. T. (2011) Quinolizidinone carboxylic acid selective M1 allosteric modulators: SAR in the piperidine series. *Bioorg. Med. Chem. Lett.* **21,** 1710–1715
38. Hulme, E. C., Lu, Z. L., Saldanha, J. W., and Bee, M. S. (2003) Structure and activation of muscarinic acetylcholine receptors. *Biochem. Soc. Trans.* **31,** 29–34
39. Lebon, G., Langmead, C. J., Tehan, B. G., and Hulme, E. C. (2009) Mutagenic mapping suggests a novel binding mode for selective agonists of M1 muscarinic acetylcholine receptors. *Mol. Pharmacol.* **75,** 331–341
40. Keov, P., López, L., Devine, S. M., Valant, C., Lane, J. R., Scammells, P. J., Sexton, P. M., and Christopoulos, A. (2014) Molecular mechanisms of bitopic ligand engagement with the M1 muscarinic acetylcholine receptor. *J. Biol. Chem.* **289,** 23817–23837
41. Mistry, S. N., Valant, C., Sexton, P. M., Capuano, B., Christopoulos, A., and Scammells, P. J. (2013) Synthesis and pharmacological profiling of analogues of benzyl quinolone carboxylic acid (BQCA) as allosteric modulators of the M1 muscarinic receptor. *J. Med. Chem.* **56,** 5151–5172
42. Conn, P. J., Jones, C. K., and Lindsley, C. W. (2009) Subtype-selective allosteric modulators of muscarinic receptors for the treatment of CNS disorders. *Trends Pharmacol. Sci.* **30,** 148–155
43. Valant, C., Felder, C. C., Sexton, P. M., and Christopoulos, A. (2012) Probe dependence in the allosteric modulation of a g protein-coupled receptor: implications for detection and validation of allosteric ligand effects. *Mol. Pharmacol.* **81,** 41–52
44. Kuduk, S. D., Di Marco, C. N., Saffold, J. R., Ray, W. J., Ma, L., Wittmann, M., Koeplinger, K. A., Thompson, C. D., Hartman, G. D., Bilodeau, M.T., and Beshore, D. C. (2014) Identification of a methoxynaphtalene scaffold as a core replacement in quinolizidinone amide M1 positive allosteric modulators. *Bioorg. Med. Chem. Lett.* **24,** 1417–1420